

## Oscillatory transient regime in the forced dynamics of a spin torque nano-oscillator

Yan Zhou<sup>1</sup>, Vasil Tiberkevich<sup>2</sup>, Ezio Iacocca<sup>1</sup>, Andrei Slavin<sup>2</sup>, and Johan Åkerman<sup>1,3\*</sup><sup>1</sup> Department of Microelectronics and Applied Physics,  
Royal Institute of Technology, Electrum 229, 164 40 Kista, Sweden<sup>2</sup> Department of Physics, Oakland University, Rochester, MI 48309 USA<sup>3</sup> Physics Department, Goteborg University, 412 96 Goteborg, Sweden

We demonstrate that the transient non-autonomous dynamics of a spin torque nano-oscillator (STNO) under a radio-frequency (rf) driving signal is qualitatively different from the dynamics described by the Adler model. If the external rf current  $I_{rf}$  is larger than a certain critical value  $I_{cr}$  (determined by the STNO bias current and damping) strong oscillations of the STNO power and phase develop in the transient regime. The frequency of these oscillations increases with  $I_{rf}$  as  $\propto \sqrt{I_{rf} - I_{cr}}$  and can reach several GHz, whereas the damping rate of the oscillations is almost independent of  $I_{rf}$ . This oscillatory transient dynamics is caused by the strong STNO nonlinearity and should be taken into account in most STNO rf applications.

Interest in spin torque nano-oscillators (STNOs) [1, 2, 3, 4] is rapidly growing among researchers as these nano-scale auto-oscillating systems have fascinating nonlinear and non-trivial properties [5]. STNOs are also interesting for rf applications due to an attractive combination of their properties, such as a wide range of generated frequencies [6], fast modulation rates [7], and easy integration into the modern on-chip nano-electronic circuits.

Recently, several groups have performed studies of the forced dynamics of an STNO under the influence of external microwave current [8, 9, 10, 11]. As with other types of auto-oscillatory systems, such dynamics results in a synchronization, or injection locking, of STNO oscillations to the external signal. The classical theory of injection locking developed by Adler in 1946 [12] is typically used to analyze such experiments on STNOs. By treating the oscillator as an active element coupled to a resonant circuit, Adler obtained a simple dynamical equation for the phase difference between the auto-oscillation and the injected driving signal:

$$\frac{d}{dt} = \omega_0 - \omega_e - F \sin(\phi) \quad (1)$$

Here  $\omega_0 = \omega_e - \omega_0$  is the mismatch between the frequency of the injected signal  $\omega_e$  and the frequency of free auto-oscillations  $\omega_0$ , and  $F$  is proportional to the amplitude of the injected signal. Despite its simplicity, Eq. (1) not only describes phase-locking phenomena in a variety of different physical systems, but accounts for all major characteristics of the phase-locking process. In particular, Eq. (1) predicts the frequency interval of phase-locking  $|\omega_e - \omega_0| < F$  and stationary phase relation  $\phi = \arcsin(\omega_e - \omega_0 / F)$  between the driving signal and the locked oscillation. Additionally, it follows from Eq. (1) that the phase approaches its locked value  $\phi$  monotonically as an exponential with a time constant  $\tau = 1/(F \cos \phi)$  inversely proportional to the driving signal  $F$ .

In this Letter, we show that for sufficiently strong injected microwave current  $I_{rf}$ , or modulation depth

$m = I_{rf}/I_{dc}$  (where  $I_{dc}$  is the dc bias current), Adler's model breaks down and does not give an adequate description of the phase-locking of an STNO. The most striking discrepancies are i) pronounced transient oscillations of the STNO phase difference during its approach to phase locking, and ii) a synchronization time  $\tau_s$  which is independent of the driving amplitude  $I_{rf}$ . We will show that these qualitative features are due to the strong nonlinearity of the STNO. Additionally, we find the critical modulation depth,  $m_{cr}$ , separating Adlerian and non-Adlerian dynamics is a surprisingly small quantity. We therefore conclude that phase locking is almost always non-Adlerian in practical STNO devices.

The STNO dynamics is studied numerically within a standard macrospin approximation [10, 13, 14, 15]. The normalized (unit-length) magnetization vector  $\mathbf{m}$  of the STNO free layer obeys the Landau-Lifshitz-Gilbert-Slonzewski (LLGS) equation [14, 16]:

$$\frac{d\mathbf{m}}{dt} = -\gamma \mathbf{m} \times \mathbf{H}_{eff} + \alpha \frac{d\mathbf{m}}{dt} + \gamma \mathbf{j} \times \mathbf{m} \quad (\mathbf{m} \cdot \mathbf{p}) = 1 \quad (2)$$

Here  $\gamma = 1.76 \times 10^4$  Hz/T is the gyromagnetic ratio,  $\mathbf{H}_{eff} = \mathbf{H}_a + M_s(\mathbf{m} \cdot \mathbf{z})\mathbf{z}$  is the effective magnetic field (where  $\mu_0 H_a = 1.5$  T is the external magnetic field applied, in the studied case, along the normal  $\mathbf{z}$  to the free STNO layer and the second term is the demagnetization field with  $\mu_0 M_s = 0.8$  T being the free layer saturation magnetization),  $\alpha = 0.01$  is the Gilbert damping constant,  $\mathbf{j}$  is the spin torque magnitude defined as  $\mathbf{j} = \hbar/2eI(2\mu_0 M_s/eV)$ , where  $\hbar$  is the Planck constant,  $\mu_0 = 0.35$  is the dimensionless spin torque efficiency,  $I$  is the applied current,  $\mu_0$  is the free space permeability,  $e$  is the fundamental electric charge, and  $V = 3 \times 10^4$  nm<sup>3</sup> is the volume of the free layer. The unit vector  $\mathbf{p} = \cos(\theta_0)\mathbf{z} + \sin(\theta_0)\mathbf{x}$  in Eq. (2), which defines the direction of current spin polarization, coincides with the magnetization direction of the fixed STNO layer. In our simulations we used a tilt angle  $\theta_0 = 60^\circ$ .

For a constant dc current  $I = I_{dc}$  the last term in Eq. (2) describes an effective negative damping that com-

compensates the natural positive magnetic damping (second term on the right hand side of Eq. (2)). When the bias current  $I_{dc}$  exceeds a certain threshold value  $I_{th}$  (2.32 mA in our case), a stable precession of the magnetization vector develops in the STNO and the free-running frequency  $\omega_0$  of this precession depends on both  $H_{eff}$  and  $I_{dc}$ . In our simulations we used  $I_{dc} = 3$  mA (supercriticality parameter  $\mu = I_{dc}/I_{th} = 1.29$ ), in which case the free STNO frequency was  $\omega_0/(2\pi) = 25.3$  GHz.

In the forced regime, when in addition to the bias current  $I_{dc}$  the STNO is driven by an injected microwave current  $I_{rf}$ , i.e.  $I(t) = I_{dc} + I_{rf} \sin(\omega_e t)$  with  $\omega_e$  close to  $\omega_0$ , the STNO may phase-lock to  $I_{rf}$ . In the phase-locked regime the generated STNO frequency becomes exactly equal to  $\omega_e$  and a fixed (independent of the initial conditions) phase difference  $\phi_0$  develops between  $I_{rf}$  and the STNO oscillation.

The results of the numerical simulations describing the STNO approach to phase-locking are shown in Fig. 1 for various  $I_{rf}$  amplitudes. The STNO was first prepared in a free-running state ( $I_{rf} = 0$ ) for 50 ns to achieve a stable free-running regime. At  $t = 0$  the microwave current  $I_{rf}$  was switched on with  $\omega_e = \omega_0$ . Since  $\omega_e$  and  $\omega_0$  coincide, the phase locking manifests itself only by establishing a fixed phase relations between these oscillations. Fig. 1 (a) shows the time dependence of  $\cos(\phi(t)) = m(t) \cdot p(t)$  (which is proportional to the STNO output signal) for the modulation depth  $\mu = I_{rf}/I_{dc} = 0.5$ . One can clearly see a transient beating of the envelope of the STNO signal, which indicates an oscillatory approach to the phase locking. This oscillatory approach is shown explicitly in Fig. 1 (b), where we plot the time dependence of the phase difference  $\psi(t) = \phi(t) - \phi_e(t)$  between the STNO phase  $\phi(t) = \arctan(m_y/m_x)$  and the phase of the external signal  $\phi_e(t)$  for several values of the modulation depth  $\mu$ .

We first note that the stationary value of the phase difference is substantially different from zero ( $\phi_0 \approx 90^\circ$ ) in contrast with what one would expect from Eq. (1) for  $\omega_e = \omega_0$ ,  $\phi_0 = 0$ . This significant intrinsic phase shift [10, 17] is caused by the strong nonlinearity of the STNO generation frequency [5]. One can also see from Fig. 1 (b) that the transient dependence  $\psi(t)$  is monotonic only for extremely small values of  $\mu$ , whereas for all the reasonable modulation depths strong oscillations of phase develop in the transient regime. The critical modulation depth, separating regions of the monotonic (Adlerian) and non-monotonic (non-Adlerian) dynamics is as small as  $\mu_{cr} = 0.0012$  (curve 2 in Fig. 1 (b)).

Another striking feature of the non-Adlerian transient regime is the very weak dependence of the synchronization time (the time needed to achieve the locked state) on the normalized driving amplitude  $I_{rf}$ . For example, the envelopes of the curves 3 and 4 in Fig. 1 (b) have essentially the same time constant  $\tau_s$ , whereas the classical Adler's model Eq. (1) predicts that the time constant in these two cases should differ by a factor of 10.

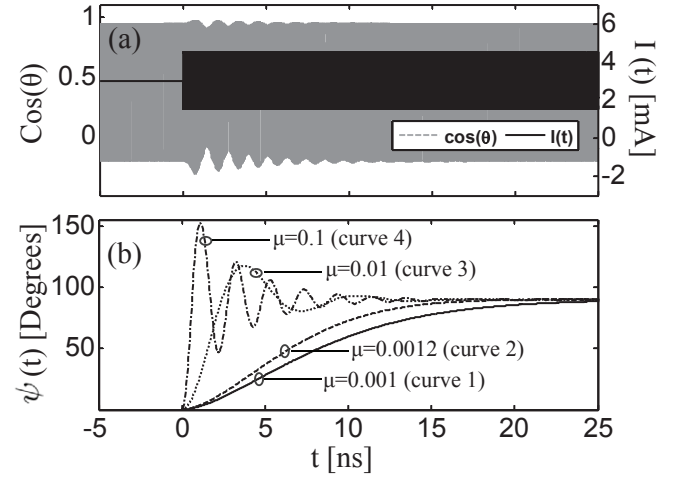


FIG. 1: (a) Time dependence of the STNO signal  $\cos(\phi(t)) = m(t) \cdot p(t)$  and (b) transient behavior of the phase difference between the STNO signal and  $I_{rf}$  after  $I_{rf}$  was switched on at  $t = 0$ .  $\mu = I_{rf}/I_{dc} = 0.5$  in (a) and  $\mu = 0.001, 0.0012, 0.01$ , and  $0.1$  for curves 1{4, respectively, in (b).

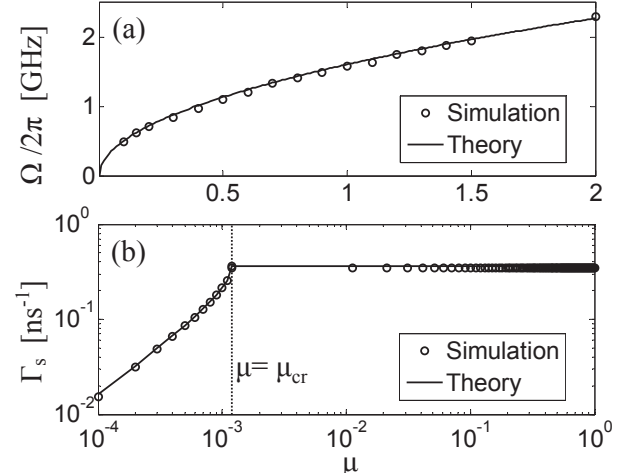


FIG. 2: Dependence on  $\mu$  of (a) the frequency of the transient STNO phase oscillations  $\Omega$ , and (b) its decay constant  $\Gamma_s$ . Points { results of numerical simulations of Eq. (2); solid lines { analytical expressions Eq. (8) and Eq. (9). The vertical line indicates the critical modulation depth  $\mu_{cr}$ .

The non-Adlerian STNO dynamics are further illustrated in Fig. 2, where we show the dependence of the frequency of the transient phase oscillations  $\Omega$  (panel (a)) and the decay constant  $\Gamma_s = 1/\tau_s$  of these oscillations (panel (b)). One can see that  $\Omega$  increases with  $\mu$  and reaches GHz values for accessible modulation depths  $\mu > 0.5$ . The decay rate  $\Gamma_s$  increases approximately linearly with  $\mu$  (following the Adler's model Eq. (1)) only for  $\mu < \mu_{cr}$ , whereas in the non-Adlerian region  $\mu > \mu_{cr}$  it remains virtually constant.

The results shown in Fig. 1 and Fig. 2 clearly demonstrate that the STNO behavior in the transient phase-

locking process can not be described by a classical Adler's model Eq. (1). Although the transient oscillations may not be visible in locking experiments performed in a stationary regime, they may significantly influence the STNO operation in applications where ultra-fast transitional dynamics are important. For instance, Fig. 2(b) shows that the synchronization time constant  $\tau_s = 1/\gamma_s$  cannot be reduced below 3 ns by increasing the amplitude of the injected current, which may limit the operational speed of STNOs as ultra-fast signal modulators.

To understand the origin of the non-Adlerian dynamics discussed above we note that STNOs, in contrast to the majority of conventional auto-oscillators, demonstrate a strong dependence of the generated frequency,  $\omega(p)$ , on the generated power  $p$  [5]. As a result, even small power fluctuations  $p = p_0 + \delta p$  from the free-running power  $p_0$  may result in significant deviations of the generated frequency  $\omega(p) = \omega_0 + N \delta p$  (here  $N = d\omega(p)/dp$  is the nonlinear frequency shift coefficient). Equations describing STNO phase locking that also take into account power fluctuations have been derived in [5] and can be written as:

$$\frac{d\phi}{dt} = \omega_0 - \omega(p) + F \sin \phi + N \delta p; \quad (3a)$$

$$\frac{dp}{dt} = -\gamma_p p + 2p_0 F \cos \phi; \quad (3b)$$

Here  $\phi(t) = \omega_0 t - \omega(p)t$  is the phase difference between the STNO signal and the external signal,  $F$  is the normalized external signal amplitude, and  $\gamma_p$  is the damping rate of power fluctuations. For the geometry studied here, all the parameters of Eqs. (3) can be calculated analytically [5] to give:  $p_0 = (1/4)I_H^2/(2I_M)$ ,  $N = 2I_M$ ,  $\gamma_p = I_H/(1/4)$ ,  $F = I_H \tan(\phi_0)/(4p_0)$ , where  $I_{sc} = I_{th}$  is the supercriticality parameter,  $I_H = j j(H_a - M_s)$  is the ferromagnetic resonance (FMR) frequency, and  $I_M = j j M_s$ , and these expressions are valid for moderate supercriticalities  $I_{sc} > 1.5$ . For a linear ( $N = 0$ ) oscillator Eq. (3a) coincides with the Adler's model Eq. (1).

The stable stationary (phase-locked) solution of Eqs. (3) has the form

$$\phi_0 = \arctan\left(\frac{\gamma_p}{N}\right) - \arcsin\left(\frac{F}{F_0}\right); \quad (4a)$$

$$p_0 = p_0 \frac{1 + \frac{F^2}{F_0^2}}{(1 + \frac{F^2}{F_0^2})^{1/2}}; \quad (4b)$$

where  $\gamma = N p_0 / \gamma_p$  is the dimensionless nonlinearity parameter (in our case  $\gamma = 100$ ) and  $F_0 = 1 + \frac{F^2}{F_0^2}$  is nonlinearity-enhanced frequency interval of phase-locking [18]. The first term in Eq. (4a) describes the above mentioned intrinsic phase shift of a strongly nonlinear STNO.

By linearizing Eqs. (3) near the solution, Eqs. (4), one can find the decay rate,  $\gamma_s$ , of phase and power deviations

from the stationary phase-locked state:

$$\begin{pmatrix} \delta\phi \\ \delta p \end{pmatrix} = \begin{pmatrix} -\gamma_p & 2F \cos \phi_0 \\ 2\gamma_p F \sin \phi_0 & -\gamma_p \end{pmatrix} \begin{pmatrix} \delta\phi \\ \delta p \end{pmatrix} \quad (5)$$

For a quasi-linear ( $N = 0$ ), or Adlerian, auto-oscillator, Eq. (5) gives  $\gamma_1 = 2\gamma_p$  and  $\gamma_2 = F \cos \phi_0$ . The decay rate  $\gamma_1$  describes the damping rate of the power deviations  $\delta p$ , whereas the rate  $\gamma_2$  corresponds to the decay of the pure phase deviations  $\delta\phi$ . The synchronization time  $\tau_s = 1/\gamma_s$  quantifies the overall time needed to reach a phase-locked state. For realistic parameters  $\gamma_p \ll F$  so the locking time of an Adlerian oscillator is determined by the transient phase dynamics and is given by  $\tau_A = 1/(F \cos \phi_0) = 1/F$ .

To analyze the case of a strongly nonlinear ( $j j > 1$ ) STNO, we note that in this case one can neglect  $F \cos \phi_0$  and simplify Eq. (5) to

$$\begin{pmatrix} \delta\phi \\ \delta p \end{pmatrix} = \begin{pmatrix} -\gamma_p & 2F \\ 2\gamma_p F & -\gamma_p \end{pmatrix} \begin{pmatrix} \delta\phi \\ \delta p \end{pmatrix} = \begin{pmatrix} -\gamma_p & 2F \\ 2\gamma_p F & -\gamma_p \end{pmatrix} \begin{pmatrix} \delta\phi \\ \delta p \end{pmatrix}; \quad (6)$$

where the critical signal amplitude is  $F_{cr} = \gamma_p/(2 \sin \phi_0)$  or, in terms of the modulation depth of the above considered STNO with a perpendicularly magnetized free layer can be expressed as

$$F_{cr} = \frac{\gamma_p}{2 \sin \phi_0} \left( \frac{1}{\tan \phi_0} \right)^{1/2} \frac{2I_H}{I_M} = 0.0012; \quad (7)$$

For modulation depths  $F > F_{cr}$  the decay rates become complex (see Eq. (6)), and describe an oscillatory approach to the phase-locked state. The frequency of these transient oscillations is given by

$$\omega_s = \frac{\gamma_p}{2} \frac{1}{F_{cr}} \quad (8)$$

and is shown as a solid line in Fig. 2(a) for the calculated value  $\gamma_p = 0.36 \text{ ns}^{-1}$ . One can see an excellent agreement between the numerical and analytical results.

The decay constant  $\tau_s$  of the phase oscillation is given by the smallest of the  $\gamma_s$ 's in Eq. (6) when both of them are real (Adlerian regime), and is equal to the real part of the  $\gamma_s$ 's, when they are complex (non-Adlerian regime):

$$\gamma_s = \begin{cases} \gamma_p & \text{if } F < F_{cr} \\ \frac{\gamma_p}{2} \frac{1}{F_{cr}} & \text{if } F > F_{cr} \end{cases}; \quad (9)$$

The dependence of Eq. (9) is shown as a solid line in Fig. 2(b), and the agreement between the simulations and the analytical calculations is again remarkable.

Thus, our analysis explains the observed non-Adlerian behavior of the transient STNO phase-locking as a result of a nonlinear coupling between the power and phase fluctuations, and provides quantitative expressions for both

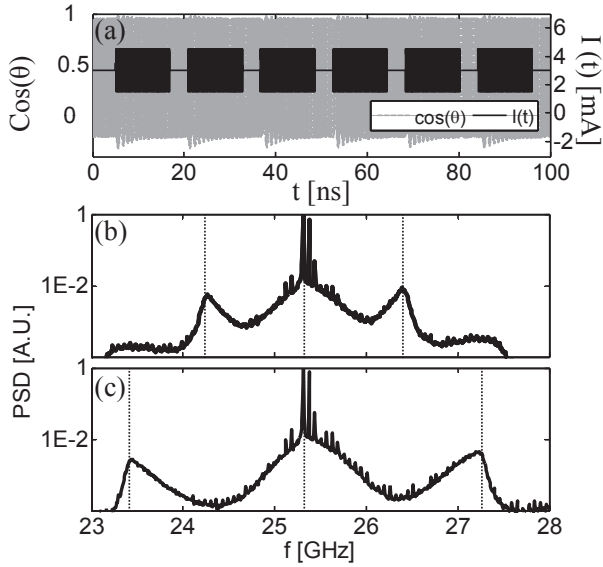


FIG. 3: Phase-locking of an STNO to a pulsed microwave signal with the repetition period of 16 ns. (a) Time dependence of the STNO signal for  $\mu = 0.5$ . (b) Spectrum of the STNO oscillations in (a). (c) Same as (b) but for  $\mu = 1.5$ . Vertical lines in (b) and (c) indicate the free-running frequency  $f_0$  and expected positions of the sidebands  $f_0 \pm n f_{rep}$ . (Other narrow sidebands are due to the direct frequency modulation at the pulse repetition rate.)

the frequency Eq. (8) and damping rate Eq. (9) of the transient phase oscillations.

We would also like to stress that the critical modulation depth  $\mu_{cr}$ , defining the boundary between the Adlerian and non-Adlerian dynamics (see Eq. (7)), is generally a small quantity, since  $\mu_{cr} \ll 1$ . Consequently, the critical microwave current  $I_{cr} = \mu_{cr} I_{dc}$  is typically of the order of 1 A, which is much smaller than the typical injection currents used in experiments. In other words, phase locking of STNOs almost always takes place in the non-Adlerian regime.

We finally suggest a way to observe the transient phase oscillations of an STNO experimentally. If the injected current is pulsed with the repetition rate of the order of  $1/\tau_p$ , large sidebands at the frequencies  $f_0 \pm n f_{rep}$  should appear in the spectrum of the STNO oscillations. Since the transient frequency  $\omega_{tr}$  may be significantly larger than the STNO generation linewidth, both the position and shape of these sidebands can be measured experimentally, providing important information about such intrinsic STNO parameters as the nonlinear frequency shift  $N$  and the damping rate  $\gamma_p$  of power fluctuations. In Fig. 3 we show the results of numerical simulations of an STNO subjected to a pulsed rf driving signal with a repetition period of 16 ns. Fig. 3(a) shows the temporal profile of the STNO signal for a modulation depth of  $\mu = 0.5$  demonstrating well-resolved intrinsic oscillations of the STNO power. Fig. 3(b) and (c) show the spectrum of STNO

oscillations for two values of the modulation depth  $\mu$ . One can clearly see the sidebands caused by the intrinsic transient STNO phase oscillations and their expected dependence on the modulation depth.

In conclusion, we have shown that the transient forced dynamics of an STNO for a sufficiently strong external signal cannot be described by the classical Adler's model. The reason for this non-Adlerian behavior is the strong nonlinearity of the STNO generation frequency, which couples power and phase fluctuations. As a result, strong phase oscillations in the GHz frequency range develop during the transient regime of phase-locking. The same nonlinear mechanism determines the lower limit for the STNO synchronization time (of the order of the characteristic decay time  $\tau_p$  of the STNO power fluctuations) and will, likely, limit the maximum speed of the STNO frequency modulation.

We thank S. Bonetti for fruitful discussions. We gratefully acknowledge financial support from The Swedish Foundation for strategic Research (SSF), The Swedish Research Council (VR), the Goran Gustafsson Foundation, by the Contract no. W 56H ZV-09-P-L564 from the U.S. Army TARDEC and RDECOM, by the Grant no. ECCS-0653901 from the National Science Foundation of the USA. Johan Akerman is a Royal Swedish Academy of Sciences Research Fellow supported by a grant from the Knut and Alice Wallenberg Foundation.

Electronic address: zhouyan@kth.se

Electronic address: akerman1@kth.se

- [1] J. A. Katine, F. J. Albert, R. A. Buhrman, E. B. Myers, and D. C. Ralph, Phys. Rev. Lett. 84, 3149 (2000).
- [2] D. Houshamdine et al, Nat. Mater. 6, 447 (2007).
- [3] J. A. Katine and E. E. Fullerton, J. Magn. Magn. Mater. 320, 1217 (2008).
- [4] D. C. Ralph and M. D. Stiles, J. Magn. Magn. Mater. 321, 2508 (2009).
- [5] A. Slavin and V. Tiberkevich, IEEE Trans. Magn. 45, 1875 (2009).
- [6] S. Bonetti et al, Appl. Phys. Lett. 94, 102507 (2009).
- [7] M. R. Puffall et al, Appl. Phys. Lett. 86, 082506 (2005).
- [8] W. H. Rippard et al, Phys. Rev. Lett. 95, 067203 (2005).
- [9] Z. Li, Y. C. Li, and S. Zhang, Phys. Rev. B 74, 054417 (2006).
- [10] Y. Zhou et al, J. Appl. Phys. 101, 09A510 (2007).
- [11] B. Georges et al, Phys. Rev. Lett. 101, 017201 (2008).
- [12] R. Adler, Proc. IRE 34, 351 (1946).
- [13] J. Z. Sun, Phys. Rev. B 62, 570 (2000).
- [14] J. Xiao, A. Zangwill, and M. D. Stiles, Phys. Rev. B 72, 014446 (2005).
- [15] Y. Zhou et al, Appl. Phys. Lett. 92, 262508 (2008).
- [16] J. C. Slonczewski, J. Magn. Magn. Mater. 159, L1 (1996).
- [17] Y. Zhou et al, Appl. Phys. Lett. 92, 092505 (2008).
- [18] A. N. Slavin and V. S. Tiberkevich, Phys. Rev. B 72, 094428 (2005).